Equator crossing times for NOAA satellites

Alexander Ignatov* and Istvan Laszlo

NOAA/NESDIS, Office of Research and Applications, 5200 Auth Road, Camp Springs, MD 20746

ABSTRACT

The local Equator Crossing Times (EXT) of all NOAA platforms have been summarized as a function of time and approximated analytically. The fit equations (superposition of two harmonic terms, with platform-specific amplitudes, frequencies, and phases) accurately reconstruct all past EXTs to within ±2 min and also allow extrapolation in time. Fit equations are summarized and used to predict the future EXT evolution. This information is important for generation of meaningful environmental and stable climate data records from data of all radiometric sensors onboard NOAA platforms.

Keywords: NOAA, equator crossing time, orbital drift.

1. INTRODUCTION

Since 1978, the TIROS-N (TN) (TIROS-N, NOAA-6, 7, 12) and Advanced TIROS-N (ATN) (NOAA-8, 9, 10, 11, 13, 14, 15, 16, 17) series of NOAA polar orbiting satellites have become an indispensable source of unique global meteorological and climatological information about the Earth[1-4]. The NOAA satellites have been designed to be sun-synchronous. However, their orbits change in time. This "orbital drift" causes a platform to systematically progress through different phases of the solar illumination and diurnal cycle of the underlying surface and atmosphere, thus modulating radiances measured by every single instrument onboard NOAA platforms and affecting meteorological and climate products derived from them. Examples are found in the literature for the Advanced Very High Resolution Radiometer, AVHRR[5-14], the Solar Backscatter Ultraviolet Radiometer, SBUV[15-16], and the TIROS Operational Vertical Sounder[17-22]. The TOVS consists of three instruments: the High-resolution Infrared Radiation Sounder, HIRS, the Microwave Sounding Unit, MSU, and the Stratospheric Sounding Unit, SSU.

The change in the local solar time (LT) of observation is closely tracked by the changes in LT when a platform crosses the equator (Equator Crossing Time, EXT). In some of the studies cited above, limited time series of the NOAA EXTs have been plotted for selected portions of active phases of some NOAA platforms. This paper provides a complete systematic summary of the EXT for all the TN/ATN platforms. It also offers convenient analytical fits for the NOAA platforms, for useful insight into the mechanisms of their EXT evolution and easy practical use. The fit equations are accurate enough to reconstruct the historical EXT data for different NOAA platforms and predict their future evolution.

2. ORBITAL CONFIGURATION AND EQUATOR CROSSING TIME

NOAA strives to keep at least two platforms in space at all times by launching new satellites to replace the aged ones. The two orbits have been carefully chosen to take four measurements a day approximately equidistant in time, at the same local solar time (LT) day after day, to provide for consistent scene illumination (in the solar reflectance bands) or segment of diurnal cycle (in the Earth emission bands). One platform is termed *morning* and the other *afternoon*, with orbital planes about 90° (six hours) apart along the approximate north-south axis. The *afternoon* satellites are launched in an ascending (northbound) orbit, with

* Alex.Ignatov@noaa.gov; phone (301)763-8053 ×190; fax (301)763-8572

Applications with Weather Satellites II, edited by W. Paul Menzel, Toshiki Iwasaki,
Proceedings of SPIE Vol. 5658 (SPIE, Bellingham, WA, 2005)
0277-786X/05/$15 · doi: 10.1117/12.577948

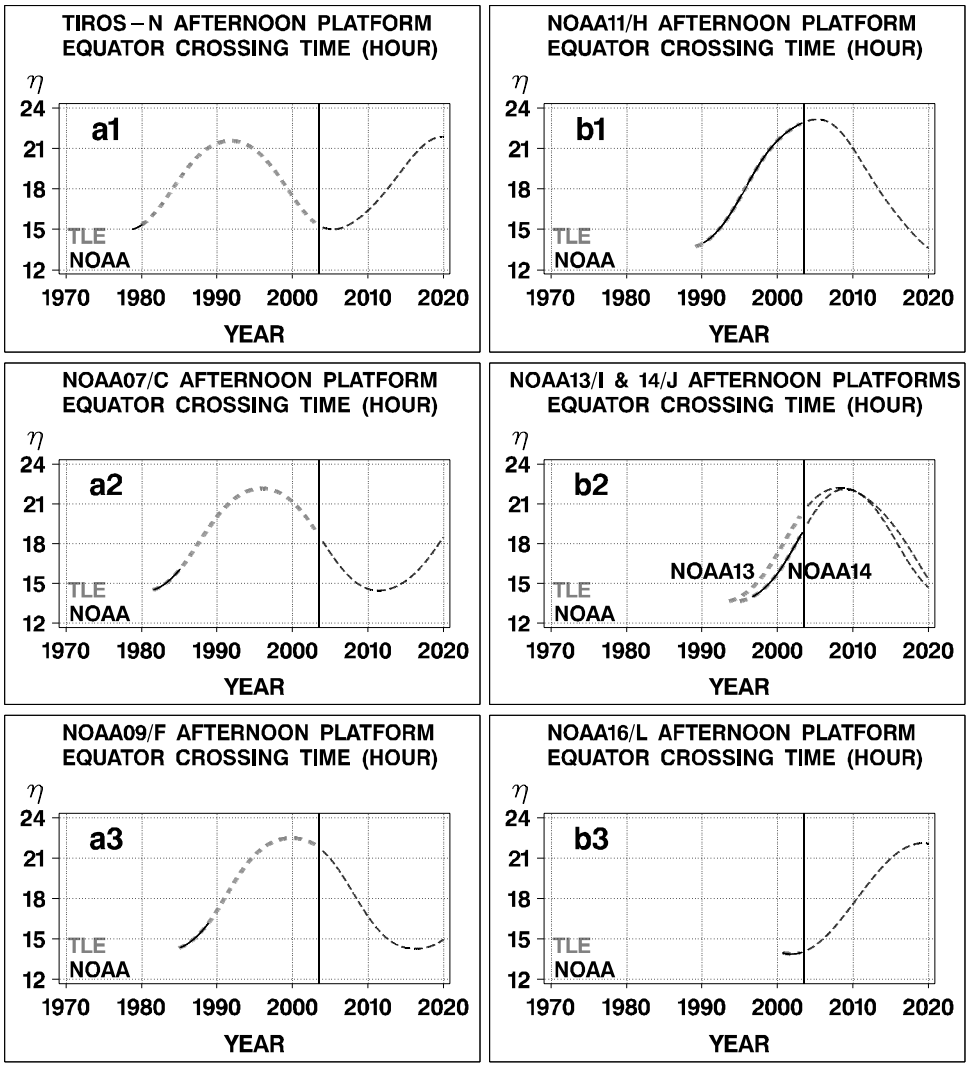

Figure 1. Local Equator crossing time, EXT (ascending/northbound node), η (h), for the seven NOAA *afternoon* platforms. (Note that NOAA-13 failed shortly after launch, and was replaced by NOAA-14. The two "twin" platforms are shown in one panel, b2). Dashed grey: the two-line element (TLE) data. Solid black: the NOAA data. Dashed black: extrapolation of the EXT based on fit Eq.(1) and data in Table 1. Solid vertical lines separate the past EXTs prior to 2003, and their future projection beyond 2004.

an EXT (η) of ~1500 (TIROS-N), ~1430 (NOAA-7, -9), ~1330 (NOAA-11, -14), or ~1400 (NOAA-16). These orbits descend back from north to south on the dark side of Earth at (η-12)~0300, 0230, 0130, or 0200, respectively. The *morning* satellites descend from north to south at η~0730, and ascend from south to north in the local evening, at (η+12)~1930. NOAA-17 is the first *mid-morning* satellite, with descending (southbound) node passing at η~1000, and ascending (northbound) node occurring at (η+12)~2200. Note that the above EXTs are but target overpass times at launch, whereas the actual EXTs systematically change during satellite lifetime as discussed below. Whatever the evolution of the EXT during the lifetime of a platform, its *morning* or *afternoon* attribute designated at launch remains unchanged.

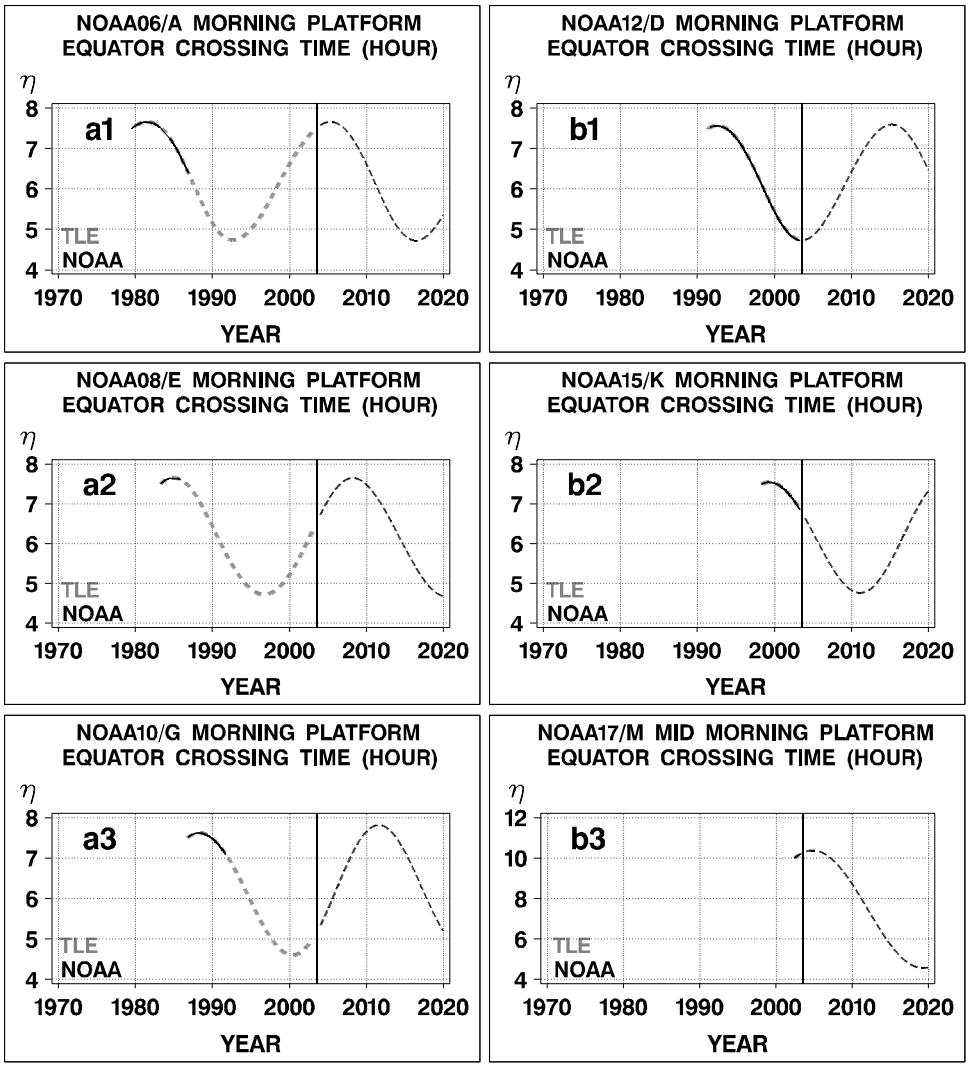

Figure 2. Same as in Figure 1, but for the six *morning* NOAA platforms (descending/southbound node).

3. DATA

NOAA uses the Brouwer-Lyddane orbit prediction package[25-26] to calculate, for each orbit, the longitude of the point at which the satellite crosses the plane of Equator in south to north direction (this point is called the *ascending node*, AN), λ_{AN} (°) and the respective AN time, T_{AN} (in Coordinated Universal Time, UTC), from which the local EXT, η, is calculated as $\eta = T_{AN} - \lambda_{AN}/15°$ [27]. Historical NOAA ephemeris files for the operational phase of each platform are available on the web in different formats and have non-uniform quality.

The U.S. Space Command (USSPACECOM; formerly the North American Aerospace Defense Command, NORAD), which is in charge of monitoring the motion of all orbital targets near Earth, produces the two-line-element (TLE) dataset. The TLE data for the full lifecycle of all NOAA platforms are available from various Internet sites. In this study, data of http://celestrak.com are used. They are available from 1980-onward in a consistent format, and exhibit few outliers. Note that in contrast to NOAA data, the TLE

calculations are run on a per need basis rather than for every orbit. Reference times (epoch) at which the TLE data are reported were chosen to be the same T_{AN} as in the NOAA data. This fact is essential as it greatly simplifies the calculation of the EXT from the TLE. Among other parameters, the TLE files report the right ascension of the AN (Ω) for a platform defined as the angle between the vernal equinox and the AN. The longitude of the equator crossing is obtained by subtracting the Greenwich mean sidereal time, Θ (expressed as the angle between the vernal equinox and the Greenwich meridian) from Ω: $\lambda_{AN}=\Omega-\Theta$, and the local standard time of the equator crossing, η, is subsequently calculated as explained above. The TLE data have been compared with the NOAA data and show excellent agreement.

4. RESULTS

Figures 1 and 2 plot the EXTs for the seven *afternoon* (ascending node; subtract 12h for the descending node) and six *morning* (descending node; add 12h for the ascending node) platforms, respectively. (Note that NOAA-13 experienced a power loss due to a circuit failure shortly after launch and NOAA-14 was launched to replace it. These "twin" platforms are combined in the panel b2 of Figure 1.) As of the time of this writing, all thirteen TN/ATN platforms continue to be in orbit, albeit some of them stopped sending data to Earth years ago. The TLE data are available for the full life cycle of each platform, with the exception of TIROS-N, which was launched in October 1978. Here, NOAA data are available through January 1980 and TLE data from January 1980 onward. As mentioned above, the NOAA data cover only the active portion of a platform's life (cf. left panels of Figures 1 and 2). In the overlapping periods, the two EXTs (derived from the TLE and NOAA data) agree within a few seconds.

The *afternoon* platforms are typically launched with η~1400, and begin drifting to later in the afternoon immediately thereafter. Their EXTs reach a maximum of η_{max}~2200 after ~15 years in orbit, and then drift back to a η_{min}~1400 in the next 15 years or so. The NOAA-16 is slightly different as its orbit was "stabilized", i.e. phased in such a way that its EXT first made a ~1.5-year long motion toward noon, before it started drifting toward later times in the same way as the previous *afternoon* platforms did. The idea of re-phasing the afternoon orbit has been a subject of discussion in the remote sensing community for a long time[5]. There is a risk for a platform to drift too far back in time, due to imprecise initial orbital conditions, possibly ruining the power system due to the increased angle of incidence of the Sun on the solar panels[5]. This risk was not minimized until very recently, when the launching rockets became accurate enough to provide highly predictable orbits. For all afternoon platforms, the range is $\delta\eta=\eta_{max}-\eta_{min}$~8h, and is centered about η~0600/1800 (descending/ascending orbits, respectively).

The *morning* orbits all appear to be "stabilized". Launched around η~0730, they first briefly drift forward in time, before drifting back to η~0430 and then returning to η~0730 again. The full cycle takes about T~24 years, and the range is $\delta\eta=\eta_{max}-\eta_{min}$~3h centered about 0600/1800 (descending/ascending orbits, respectively).

The NOAA-17/M was put into an unusual *mid-morning* orbit with an EXT of η~1000 (southbound/ descending node). Its full period is T~28 years, and the range, $\delta\eta$~6h, centered about 0730/1930 (see next section for explanation on how its T and $\delta\eta$ were determined). The NOAA-17 "average" time is thus shifted with respect to both afternoon and morning platforms by 1h 30min, and its range, $\delta\eta$~6h, falls between the *morning* ($\delta\eta$~3h) and *afternoon* ($\delta\eta$~8h) values.

5. FITTING NOAA EXT`S AND PREDICTING THEIR FUTURE EVOLUTION

Approximating time series of the historical EXT with simple analytical functions is useful to succinctly represent them and predict future evolution. To choose an appropriate form of the fit equation, recall that, for a given orbital period, the local EXT of a satellite is determined by the position of its orbital plane in space relative to the direction of the Sun, measured by the right ascension of ascending node (Ω). The orbital plane

Table 1. Fit parameters in equation (2) for NOAA afternoon platforms.

	JD_o	η_o, h	α_1, h	ω_1, JD^{-1}	ϕ_1, rad	α_2, h	ω_2, JD^{-1}	ϕ_2, rad	σ_η, s
TIROS-N	2444242	18.350	3.367	6.093e-4	5.247	0.150	1.551e-3	4.438	11
NOAA-07	2444779	18.311	3.972	5.419e-4	5.008	0.140	1.511e-3	3.183	21
NOAA-09	2446047	18.367	4.312	5.160e-4	5.064	0.207	1.506e-3	2.969	25
NOAA-11	2447583	18.258	4.935	4.989e-4	5.036	0.164	1.754e-3	2.244	7
NOAA-13	2449209	17.913	4.410	5.603e-4	4.841	0.122	1.811e-3	1.220	3
NOAA-14	2449717	17.759	4.348	5.718e-4	4.809	0.224	1.540e-3	1.451	3
NOAA-16	2451809	18.099	4.141	4.955e-4	4.531	0.212	3.129e-4	3.404	3

is moving, due primarily to gravitational perturbations. Kaula (2000)[28] provides analytical expressions for the rate of change in Ω due to the secular (linearly proportional with time) and periodic perturbations caused by the non-spherical gravitational field of Earth. Following Kaula's method and integrating the Lagrange equations (Kaula's Eq. 3.38) with the disturbing function (Kaula's Eq. 3.70) and assuming that the longitude of the ascending node, the argument of perigee and the mean anomaly are all linear functions of time and that the remaining three orbital elements (the semimajor axis, eccentricity and inclination) are constant, one can write the change δΩ as:

$$\delta\Omega = A(t-t_o) + \sum_{l=1}^{\infty}\left\{B_l \cos\left[p_l\,(t-t_o)+q_l\right] + C_l \sin\left[p_l\,(t-t_o)+q_l\right]\right\} \tag{1}$$

Here t is the time elapsed since a chosen reference time t_0. The constants A, B_l, C_l, p_l, and q_l are functions of the orbital elements. Note that the other astronomical objects in the Solar system (chiefly, the Sun itself) affect the EXT perturbations as well. Their combined effect can still be described in a form of Eq.(1), but with a different set of parameters.

The orbits of sun-synchronous satellites are designed in such a way that the first (secular) term in δΩ, the dominant part of which is due to the equatorial bulge of the Earth, matches the average rate of the Sun's motion projected on the equator: A≈360°/365.25 days. With respect to this rotating orbital plane, the changes exhibited in the EXT are then represented by the second (periodic) term. We have used this periodic term to guide us in the construction of the function for the fitting. Eq.(1) suggests that this term is expressed as an infinite series of sums of cosine and sine functions, with the same frequency and phase for a given index l. To restrict the number of parameters needed in the fit, we replace the infinite series with a sum of a constant and one or two harmonic terms, H_1 and H_2, with different frequencies and phases, and arrive at

$$\eta = \eta_o + \alpha_1 \times \sin\left[\omega_1 \times \left(JD - JD_o\right) + \phi_1\right] + \alpha_2 \times \sin\left[\omega_2 \times \left(JD - JD_o\right) + \phi_2\right], \tag{2}$$

that can be viewed as a formal mathematical approximation of a periodic function with one or two Fourier terms. A secular term, similar to the $A(t-t_o)$ term in Eq.(1) representing residual of the linear drift in the EXT with time, was also tested in Eq.(2), but was found to be statistically insignificant (indicating highly accurate sun-synchronization of the NOAA orbits) and, therefore, is not included. In Eq.(2), the η_o has a meaning of an average EXT, around which the actual EXT oscillates; the α_i, ω_i, and ϕ_i are the amplitude, frequency, and phase of the respective harmonics (i=1,2), and the JD is the Julian Day (algorithm for calculating JD is available e.g. from Ref. 27); JD_o is the first JD for which the TLE data were available for a platform. (Note: this should not be confused with the launch date).

The JD_o and the fit parameters for the *afternoon* and *morning* platforms are summarized in Tables 1 and 2. The RMSE for approximating the historical EXTs with the fit equations, σ_η, is always less than 30 seconds and the maximum error never exceeds 2 min. These errors could be further reduced, if needed, by adding a

Table 2 Fit parameters in equation (2) for NOAA morning platforms. *Note that NOAA-17 is a mid-morning platform and, therefore, its fit parameters differ from the other morning platforms.

	JD_o	η_o, h	α_1, h	ω_1, JD^{-1}	ϕ_1, rad	α_2, h	ω_2, JD^{-1}	ϕ_2, rad	σ_η, s
NOAA-06	2444242	6.226	1.458	7.268e-4	1.244	0.080	1.443e-3	5.267	29
NOAA-08	2445422	6.156	1.470	7.310e-4	1.134	0.037	1.650e-3	0.092	7
NOAA-10	2446691	6.176	1.543	7.320e-4	1.159	0.103	1.146e-3	4.123	7
NOAA-12	2448391	6.178	1.421	7.613e-4	1.272	0.041	1.637e-3	4.509	3
NOAA-15	2450947	6.169	1.399	7.507e-4	1.260	0.040	1.356e-3	3.404	2
NOAA-17*	2452450	7.489	2.810	6.000e-4	1.040	0.130	3.267e-4	3.324	1

third harmonic in Eq.(2). Using only one harmonic in place of two, on the other hand, leads to a less accurate fit (error increases by a factor of 3-4). It is thus concluded that Eq.(2) is sufficiently accurate for our purpose. Note that in the calculation of Tables 1 and 2, the (real value) JD in Eq.(2) was specified from the exact UTC of the satellite equator crossing for the ascending node, T_{AN}, which is not available to the reader of this paper. Numerical estimates show that specifying the (integer value) JD for the center of a day leads to worst-case error in the EXT of up to a few seconds, which is typically smaller compared to the fit error and, therefore, not critical for practical use of Eq.(2). For example, the EXT for TIROS-N at midday (UTC=1200) 25 November 1986 (JD=2446760) and calculated using Eq.(2) and data in Table 1 is η=20.091h. The TLE result for the orbit passing at UTC~0327 on that day is η=20.09157h, a ~2 s difference from the predicted value.

In Eq.(2), η_o is the average EXT. It ranges from η_o~1745 to η_o~1820 for the *afternoon* platforms (ascending node), and from η_o~0610 to η_o~0615 for the *morning* platforms (descending node). This means that if a consistent node is considered, the average EXT is η_o~0600/1800, and approximately the same for all NOAA platforms except NOAA-17.

The first harmonic (H_1) approximates the EXT shape well. For the *afternoon* platforms, the parameters of H_1 are: α_1~3.4-4.9 h, ω_1~$(5-6)\times10^{-4}$ JD^{-1} (corresponding to a period of T_1~28-35 years), and ϕ_1~4.5-5.2. For the *morning* platforms, the parameters of H_1 are: α_1~1.4-1.5 h, ω_1~7.4×10^{-4} JD^{-1} (corresponding to a period of T_1~23 years), ϕ_1~1.1-1.3.

[To better understand these results, numerical experiments with a simple model have been done. They show that if the Earth's gravitation was the only cause of the orbital drift, the empirical periods and amplitudes should be at least an order of magnitudes smaller. It is therefore felt that the observed fit parameters and the large differences between the morning and afternoon platforms can be explained only if the effect of Sun is considered. The secular rate of Ω is very sensitive to variations in the inclination of the orbit and, for sun-synchronous orbits, the otherwise small perturbations in the inclination would build up with time (a phenomena known as "deep resonance" in orbital mechanics)[29]. The rate of change in the inclination due to the Sun depends on the desired value of EXT for the satellite[5]. Thus, it is expected that the amplitude of η will be different for the morning (EXT~0730) and the afternoon (EXT~1400) satellites.]

The accuracy of the fit is further improved by the second harmonic (H_2). The parameters of the H_2 for the *afternoon* platforms are: α_2~0.14-0.22 h, ω_2~$(1.5-1.8)\times10^{-3}$ JD^{-1} (corresponding to a period of T_2~9-11 years), ϕ_2~1.2-4.4. For the *morning* platforms, α_2~0.04-0.10 h, ω_2~$(1.1-1.6)\times10^{-3}$ JD^{-1} (corresponding to a period of T_2~11-16 years), ϕ_2~0-5.3.

All fit parameters (except for the phase of H_2) appear well reproducible from one platform to another. Note that the frequencies of H_2 for NOAA-16 and -17 are about five times lower compared to their predecessors. Additionally, the NOAA-17 average EXT η_o~0730/1930 is dramatically different from all other NOAA platforms.

Future projections (up to 2020) of the EXTs for all NOAA platforms, based on the estimated fit equations, are also plotted in Figures 1 and 2. Predictions are undoubtedly more accurate for the earlier platforms, but are deemed to be good, at least qualitatively, for the more recent platforms (such as NOAA-16 and -17) as well, based on the physical Eq.(2), whose parameters are reproducible for all similar platforms. In particular, the NOAA-16 will be flying at η~1500 by 2006, at η~1600 by 2008, and at η~1800 by 2011. The NOAA-17 EXT will reach its maximum of η_{max}~1020 by 2005, then return to the launch value of η~1000 by 2007, subsequently declining to η~0900 by 2009 and η~0800 by 2011.

6. EQUATOR CROSSING TIME AND LOCAL TIME OF OBSERVATION

When using the EXT as a proxy for the LT of satellite sensor observation, two factors should be considered. First, the LT changes systematically with latitude, due to the Earth's rotation and orbit inclination, even for nadir views. Simple geometrical considerations suggest that the local pass time at a latitude φ, $\eta_{A\varphi}$ (h), is represented for the ascending and descending branches as

$$\eta_{A\varphi} = \eta_{Ao} + \frac{\arcsin\left(\frac{\tan(\varphi)}{\tan(i)}\right)}{15°}; \qquad \eta_{D\varphi} = \eta_{Do} - \frac{\arcsin\left(\frac{\tan(\varphi)}{\tan(i)}\right)}{15°}, \tag{3}$$

respectively where i is the orbital inclination which also changes systematically over the lifetime of a platform. For NOAA platforms, a representative number of i~99.0±0.4° can be used. Note that tan(i)<0 and, therefore, on the ascending pass $\eta_{A\varphi} < \eta_{Ao}$ ($\eta_{A\varphi} > \eta_{Ao}$) to the north (south) of Equator, whereas on a descending pass, $\eta_{D\varphi} > \eta_{Do}$ ($\eta_{D\varphi} < \eta_{Do}$). In particular, the min/max latitude can be estimated from Eq.(3) as the point at which $\eta_{A\varphi} = \eta_{D\varphi}$. Recalling $\eta_{Ao} = \eta_{Do} + 12$, one obtains $\varphi_{max}/\varphi_{min} = \pm(180° - i) \sim \pm 81°$. This latitude is reached six hours from both η_{Ao} and η_{Do}, i.e., exactly between the two EXTs.

Equation (3) can be used for a non-scanning radiometer onboard a NOAA satellite, such as the SBUV instrument. All other radiometers (AVHRR, HIRS, MSU, and SSU) scan cross-track and, therefore, may "look" more than a thousand kilometers off nadir. Calculation of the local observation time from these sensors requires an additional correction for the scan effect.

7. CONCLUSION

The systematic changes of the local observation time during the life cycle of a platform and between different platforms are significant and should be accounted for when using multi-year time series of satellite products in long-term monitoring/climate analyses. This paper systemizes the available information on the EXT for the sun-synchronous NOAA platforms and represents it succinctly with simple analytical formulae to facilitate calculation of the past EXTs for the NOAA platforms and a prediction of their future evolution. One observation clearly emerges from our analyses is that the term "orbital degradation", commonly used in the literature on the NOAA satellites, should be avoided and a more appropriate term, such as "orbital evolution", should be used instead. Note that EXT data for the EOS and ERS sun-synchronous platforms are available from Ref. 30.

ACKNOWLEDGEMENT

Thanks go to Konstantin Vinnikov (University of Maryland, USA), E.Harrod, K.Kidwell, G.Goodrum, Dan Tarpley, Jerry Sullivan, Felix Kogan, Mike Weinreb, Shobha Kondragunta, Larry Flynn, Jim Miller,

Changyong Cao, Nick Nalli, Paul Menzel, Yan Ming Wang, Alex Kidd, and Mike Simpson (NOAA, USA) for helpful discussions and advice, and help with the NOAA equator crossing time data. This work was funded under the Integrated Program Office (NOAA/NASA/DOD), NASA EOS/CERES (NASA contract L-90987C), NOAA/NESDIS Ocean Remote Sensing and Polar Satellites Programs, and Joint Center for Satellite Data Assimilation. We are thankful to Steve Mango (IPO), Bruce Wielicki (NASA/LaRC), Eric Bayler, Al Strong, Bill Pichel, Mike Mignogno, Tom Schott, and Fuzhong Weng (NOAA/NESDIS) for their support and encouragement. Special thanks go Dennis Clark, Eric Bayler, and Al Powell (NOAA) for careful reading the manuscript, and helpful editorial suggestions. The views, opinions, and findings contained in this report are those of the authors and should not be construed as an official National Oceanic and Atmospheric Administration or U.S. Government position, policy, or decision.

REFERENCES

1. Rao, P. K. S.G.Holmes, R.K.Anderson, J.S.Winston, and P.E.Lehr, Eds, 1990: Weather Satellites: Systems, Data and Environmental Applications. AMS, Boston, MA, 503 pp.
2. Kidder, S., and T. Vonder Haar, 1995: Satellite meteorology: An introduction. Academic Press, 466 pp.
3. Cracknell, A., 1997: The Advanced Very High Resolution Radiometer. Taylor and Francis, 534 pp.
4. Cracknell, A., (Ed.), 2001: Remote sensing and climate change. Praxis Publishing, 301 pp.
5. Price, J., 1991: Timing of NOAA afternoon passes. *International Journal of Remote Sensing*, **12**, 193-198.
6. Gutman, G., and A.Ignatov, 1995: Global land monitoring from AVHRR: potential and limitations. *International Journal of Remote Sensing*, **16**, 2301-2309.
7. Privette, J., C.Fowler, G.Wick, D.Baldwin, and W.Emery, 1995: Effects of orbital drift on AVHRR products: normalized difference vegetation index and sea surface temperature. *Remote Sensing of Environment*, **53**, 164-171.
8. Brest, C., W.Rossow, and M.Roiter, 1997: Update of radiance calibrations for ISCCP. *Journal of Atmospheric and Oceanic Technology*, **14**, 1091-1109.
9. Gutman, 1999: On the monitoring of land surface temperatures with the NOAA/AVHRR: Removing the effect of satellite orbit drift. *International Journal of Remote Sensing*, **20**, 3407-3413.
10. Gutman, 1999: On the use of long-term global data of land reflectances and vegetation indices derived from AVHRR. *Journal of Geophysical Research*, **104**, 6241-6255.
11. Kogan, F., and X.Zhu, 2001: Evolution of long-term errors in NDVI time series: 1985-1999. *Advances in Space Research*, **28**, 149-153. Mears, C., M.Shabel, and F.Wentz, 2003: A reanalysis of the MSU channel 2 tropospheric temperature record. *Journal of Climate*, **16**, 3650-3664.
12. Stowe, L., H.Jacobowitz, G.Ohring, K.Knapp, and N.Nalli, 2002: The AVHRR Pathfinder Atmosphere (PATMOS) climate data set: Initial analyses and evaluations. *Journal of Climate*, **15**, 1243-1260.
13. Cao, C., J.Sullivan, E.Maturi and J.Sapper, 2004: The Effect of orbit drift on the radiometric calibration of the 3.7 μm channel of the AVHRR onboard NOAA-14 and its impact on night-time sea surface temperature retrievals. *International Journal of Remote Sensing*, **25**, *5*, 975-986.
14. Reynolds, R., C. Gentemann, and F.Wentz, 2004: Impact of TRMM SSTs on a climate-scale SST analysis. *Journal of Climate*, 17, 15, 2938-2952.
15. Flynn, L., S.Kondragunta, K.Horvath, and E.Beach, 2000: Internal validation of SBUV/2 ozone vertical profile dataset. Proc. Quadrennial Ozone Symp., Hokkaido Univ., Sapporo, Japan 3-8 July, 2000, 75-76.
16. Miller, A., R.Nagatani, L.Flynn, S.Kondragunta, E.Beach, et al., 2002: A cohesive total ozone data set from SBUV/2 satellite system. *Journal of Geophysical Research*, **107**, 4701, doi:10.1029/2001JD000853.

17. Brownscombe, J., J.Nash, G.Vaughan, and C.Rogers, 1985: Solar tides in the middle atmosphere I. Description of satellite observations and comparison with theoretical calculations at equinox. *Quarterly Journal of the Royal Meteorological Society*, **111**, 677-689.
18. Bates, J., X.Wu, and D.Jackson, 1996: Interannual variability of upper-troposphere water vapor band brightness temperature. *Journal of Climate*, **9**, 427-438.
19. Waliser, D., and W.Zhou, 1997: Removing satellite equatorial crossing time biases from the OLR and HRC datasets. *Journal of Climate*, **10**, 2125-2146.
20. Jackson, D., and J.Bates, 2001: Climate analysis with the 21-year HIRS Pathfinder radiance clear-sky data set. Proc.11th Conf. on Satellite Meteorology & Oceanography, Madison, Wisconsin, October 15-18, 2001.
21. Christy, J., R.Spencer, W.Norris, and W.Braswell, 2003: Error estimates of version 5.0 of MSU-AMSU bulk atmospheric temperatures. *Journal of Atmospheric and Oceanic Technology*, **20**, 613-629.
22. Mears C., M.Schabel, F.Wentz, 2003: A reanalysis of MSU channel 2 tropospheric temperature record. *J. Climate*, **16**, *22*, 3650-3664.
23. Menzel, P., D. Wylie, D. Jackson, and J.Bates, 2002: HIRS Observations of Clouds Since 1978. Proc. Conf. on Applications with Weather Satellites at the SPIE 3rd International Asia-Pacific Environmental Remote Sensing Symposium held in Hangzhou, China 23-27 October, 2002.
24. Vinnikov, K, and N.Grody, 2003: Global warming trend in satellite observed mean troposphere temperature. *Science*, **302**, 269-272.
25. Kidwell, K. (Ed.), 1998: "NOAA Polar Orbiter Data User's Guide (TIROS-N, NOAA-6, -7, -8, -9, -10, -11, -12, -13, and -14", U.S. Dept. of Commerce, NOAA/NESDIS, 394 pp. (Available from National Climatic Data Cenetr, 151 Patton Ave, Rm.120, Asheville, NC 28801-5001, http://www2.ncdc.noaa.gov/docs/podug/index.htm).
26. Goodrum, G., K. Kidwell, and W. Winston (Eds.), 2003: "NOAA-KLM user's guide," U.S.Dept. of Commerce, NOAA/NESDIS. (Available from National Climatic Data Center, 151 Patton Ave, Rm.120, Asheville, NC 28801-5001, http://www2.ncdc.noaa.gov/docs/klm/index.htm).
27. Duffett-Smith, P., 1988: Practical astronomy with your calculator. Cambridge Univ. Press (3rd ed), NY, 185 pp.
28. Kaula, W., 2000: Theory of satellite geodesy: Applications of satellites to geodesy. Dover Pub; Reprint Edition, 140 pp.
29. Vallado, A.D., 2001: Fundamentals of astrodynamics and applications, 2nd edition, Space Technology Laboratory, Vol. 12, Kluwer Academic Publishers, Dordrecht, The Netherlands, June 2001, 980 pp.
30. Ignatov, A., I.Laszlo, E.Harrod, K.Kidwell, G.Goodrum, 2004: Equator crossing times for NOAA, ERS and EOS sun-synchronous platforms. *International Journal of Remote Sensing*, in press.